Retinal oxygenation with conventional 100ms vs short-pulse pan-retinal laser photocoagulation

Abstract

Background: Conventional (100ms) pan-retinal photocoagulation (PRP) laser burns are larger than short-pulse (10-20ms) PRP burns. This study investigates the effect of PRP burns of different sizes on retinal oxygenation.

Methods: A mathematical model using COMSOL Multiphysics 6 was employed to create a 3D abstraction of the coupled biology of the choroid, photoreceptor, and retinal tissues. Laser burn sizes were varied in the model, specifically considering burn diameters of 500µm, 250µm, and 125µm, while keeping the total burn area constant.

Results: Total increase in retinal oxygenation was the same for different burn sizes, but the oxygen distribution differed. Smaller burns resulted in a more even lateral oxygen distribution but with reduced penetration into the inner retina.

Conclusions: Conventional and short-pulse PRP may affect retinal oxygenation differently, even when total burn area is the same. Further investigation into optimum burn size and pattern is required.

Introduction

Panretinal photocoagulation (PRP) is the standard treatment for proliferative diabetic retinopathy (PDR). The Early Treatment Diabetic Retinopathy Study (ETDRS) used a PRP protocol consisting of 1200-1600 burns of 500μm diameter and 100 ms pulse duration [1]. 1600 500 μm burns equate to $314mm^2$ or approximately one quarter of the total retinal area.

Newer laser modalities (e.g. PASCAL, Navilas) use shorter pulse durations of 10-20 ms. Short-pulse duration laser can be applied more quickly and with less discomfort than conventional laser [2,3]. An important difference between conventional and short pulse laser is the final size of the burn. Short-pulse burns shrink over time whereas conventional 100ms burns expand. After 6 months, a 400μm 20ms burn is approximately half the diameter of a 400μm 100ms burn [4]. Figure 1 illustrates the relationship between burn diameter and area – a doubling of burn diameter results in a quadrupling of the burn area.

The reduced burn size with short-pulse laser means a greater number of burns are required to achieve disease regression compared to conventional laser (e.g. ETDRS: 1600 burns, RCOphth guidelines for short-pulse burns: 2500-3500 burns for mild PDR, ~4000 for moderate PDR and ~7000 for severe PDR[5]).

The area of a short-pulse burn is approximately four times smaller than the area of a

100ms burn. If total retinal burn area were the only parameter determining laser efficacy, four times as many short-pulse burns would be needed for the same clinical effect as conventional 100ms burns. This is not observed in clinical practice. In numerous comparison trials, a similar efficacy was observed despite a smaller total burn area (total burn area calculated assuming 400μm burns shrink or expand depending on the laser pulse duration as explained above) (Table 1).

It is not understood how a similar treatment efficacy is achieved despite this difference in total burn area.

Study	PRP type	No of burns	Mean total burn area (mm^2)	Relative burn area (vs conventional PRP)
Nagpal *et al* (2010) [6]	**Conventional PRP** (Assuming 400μm burns increase in size to 500μm diameter)	1150	225	
	Short-pulse PRP (Assuming 400μm burns shrink in size to 250μm diameter)	2186	107	48%
Muraly *et al* (2011) [7]	**Conventional PRP**	1414	277	
	Short-pulse PRP	2795	137	49%
Mishahi *et al* (2013) [8]	**Conventional PRP**	1218	239	
	Short-pulse PRP	2125	104	44%
Saymenoglu *et al* (2016) [9]	**Conventional PRP**	1642	322	
	Short-pulse PRP	2885	142	44%
Nemkansky *et al* (2019) [10]	**Conventional PRP**	1685	330	
	Short-pulse PRP	2113	104	31%
ETDRS [1]		1600	314	

Table 1: Studies showing equal efficacy between conventional and short-pulse PRP in treating PDR. Total calculated burn area is significantly smaller for short-pulse laser.

PRP mechanism of action and the oxygen hypothesis

The retina has a dual oxygen supply, from the inner retinal vasculature and from the choroid. Damage to the inner retinal vasculature in diabetes can lead to retinal hypoxia, subsequent up-regulation of pro-angiogenic growth factors such as vascular endothelial growth factor and the development of PDR.

The generally accepted mechanism of action of PRP is that it reduces retinal hypoxia by increasing retinal oxygenation from the choroid. Photoreceptor inner segments are highly metabolically active and effectively act as a metabolic barrier to oxygen diffusion from the choroid into the inner retina. By destroying this metabolic barrier with PRP burns, choroidal oxygen may diffuse further into the inner retina, thus reducing inner retinal hypoxia.

This hypothesis is supported by experimental data. Experiments in animals using oxygen-sensitive electrodes showed an increase in inner retinal [11] and pre-retinal [12] oxygen tension over laser burns. In humans, Muqit *et al* used multispectral imaging to show an increase in retinal tissue oxygenation both in the retina directly above and the retina in between laser burns [4].

In this paper, we present a mathematical model to investigate the role of laser burn size on oxygen diffusion in the retina. We consider how differences in retinal oxygenation between burn sizes might relate to clinical efficacy.

Methods

The mathematical model was produced using COMSOL Multiphysics 6 and represents a 3D abstraction of the coupled biology of the choroid, photoreceptor and retinal tissues. Figure 2 illustrates a schematic diagram of the mathematical model, which is a cuboid, as both a 2D and 3D projection.

1. The Choroid is modelled as a boundary effect on the bottom of the dark blue, photoreceptor (PR) region. This PR region is modelled as a 50μm tall layer, in which the highly metabolically-active PR inner segments are contained. The choroid acts as a constant source of oxygen that can diffuse through the rest of the material. On top of this PR region is a layer that models the rest of the retina including the remaining PR layer (up to the outer nuclear layer), and the inner retina.
2. As oxygen diffuses from the choroid, through the PR layer and retina it is consumed at a rate proportional to the amount of oxygen present. Due to the distinct metabolic demands of different retinal segments, there is variability in oxygen consumption rates. The PR inner segments have very high metabolic activity, with an estimated oxygen consumption rate of 16-20 ml O_2/100mg tissue/min. This rate is notably higher than the inner retina, where the oxygen consumption measures approximately 3.5-4 ml O_2/100mg tissue/min. Reflecting this disparity, our model assumes that the oxygen consumption in the PR layer is five times greater than in the other parts of the retina [13,14]
3. Laser burns (red region) were inserted into the PR layer. Within the red burn region, the oxygen can diffuse, but it is not consumed. Burns are placed orthogonally on a square lattice. The

diameter and number of burns and the inter-burn spacing are varied throughout this investigation. Specifically, we considered burn diameters of 500μm, 250μm and 125μm. The spacing between burns was equal to the burn diameter. The number of burns was chosen to ensure that the total burn area was the same throughout all simulations (i.e. 4 x 500μm burns, 16 x 250μm burns and 64 x 125μm burns).

4. In the DR models, there was no inner retinal oxygen source, as may be seen in advanced DR with extensive capillary non-perfusion.

5. To aid the comparison between models, a model of healthy retina was constructed in which an additional source of oxygen was inserted in a thin region (25μm in thickness beginning at a depth of 80μm from the inner limiting membrane (ILM)), to model oxygen supply from the capillary plexuses in the inner retinal circulation. This layer is a simplified approximation of the inner retinal capillary plexuses.

6. The boundary conditions along the *x*- and *y*-directions are periodic. Namely, oxygen that diffuses out of the left-hand boundary of the domain appears at the right-hand boundary (and vice versa). This represents the idea that our model forms a small part of a larger repeated structure. The boundary condition on the top of the model is zero-flux, meaning that it is insulated, and no oxygen passes through the top boundary.

Various retinal oxygen parameters for different laser burn sizes were compared using this model. (Further details of the diffusion equations governing the model are provided in Supplementary file 1.)

Results

1) Total retinal oxygenation is related to total burn area and is affected minimally by changing burn size.

Figure 3 shows the average oxygen concentration across the retinal model for different burn diameters, with the healthy model (grey line) and no treatment model (dashed red line) for comparison. Total retinal oxygenation is approximately equal for each burn diameter.

2) Smaller burns give a more even lateral spread of oxygen but with less penetration into the inner retina

Figure 4A shows the retinal oxygen profile through the centre of retinal burns of 500μm, 250μm and 125μm. The solid yellow line represents the oxygen profile of the healthy model and shows a good approximation to retinal oxygen profiles observed *in vivo* [13] (see Supplementary file 1).

Figure 4B was generated by analysing the oxygen profile across the 3D model and shows oxygen plumes over retinal burns. These plumes show the volume of retina that matches or exceeds the oxygen concentration of the healthy model. Larger burns produce larger oxygen plumes that penetrate further into the inner retina. Smaller but more numerous burns give a more even lateral spread of oxygen but with less penetration into the inner retina.

3) With smaller and more numerous burns, the most oxygenated tissue is worse off (vs larger burns) but the least oxygenated tissue is better off.

Figure 5 shows the oxygen concentration along a single line at a depth (from the ILM) of 50% (125μm) and 75% (182.5μm) and running across a row of burns of various sizes. The highest oxygen concentration occurs directly over the burn and reduces with increasing distance from the centre of the burn. As burn size is reduced, the concentration curve flattens out, indicating a more even horizontal oxygen distribution.

Discussion

Our study indicates for the first time how conventional and short-pulse PRP may affect

retinal oxygenation differently. In our model, the total burn *area* was kept equal for each burn size, thus helping to determine the effect of burn *pattern* on oxygenation parameters. The total oxygen increase after PRP is the same for each burn size but this oxygen is distributed differently in the retina. Smaller and more numerous burns resulted in a more even lateral oxygen distribution when compared to larger burn sizes. This was at the cost of reduced oxygen penetration into the inner retina.
In clinical practice, PRP with smaller and more numerous burns (e.g. PASCAL laser) appears to have a similar efficacy to conventional 100ms laser despite a smaller total burn area (Table 1). This suggests that the enhanced lateral oxygen distribution predicted by our model may be important in determining treatment efficacy.

Modelling oxygenation in the diabetic retina is complex and is influenced by numerous parameters, many of which are heterogeneous or incompletely determined *in vivo*. There are geometric parameters, such as the retinal dimensions and the thickness of particular retinal layers, or kinetic parameters such as the oxygen consumption of different retinal layers and oxygen diffusion characteristics. These all contribute to the intricate nature of retinal oxygenation in the context of diabetic retinopathy and PRP. In this paper, we have used a comparative, parametric approach to make comparisons *between* burn patterns. Varying retinal geometric or oxygenation parameters will affect all burn pattern models equally and therefore the effect of the variability of these parameters on the comparison between models is minimized.

Our study, based on finite element analysis, lacks experimental validation. Current techniques for measuring retinal oxygenation in humans largely rely on differences in absorption spectra between oxy- and de-oxyhemoglobin, primarily offering data on retinal vascular oxygen concentration[15]. In contrast, animal studies have employed oxygen-sensitive phosphorescent probes, "oxyphors," compounds whose phosphorescence lifetime is sensitive to the local oxygen concentration. Use of these probes has enabled depth-specific readings of both vascular and tissue oxygen concentrations[16]. Applying this imaging approach to animal models of laser-treated diabetic retinopathy could be a way of investigating our findings experimentally.

An additional limitation of our study is that the oxygen parameters are non-dimensional and so we cannot determine the actual degree of hypoxia or increase in oxygenation with different laser patterns. This reflects the comparative, parametric approach we have taken. In this study, our intention was to understand relative differences in retinal oxygen parameters with different PRP burn configurations. Improving our conceptual understanding of the potential mechanisms of action of PRP laser in this way may guide future experimental and clinical research.

In the retina, there exists a watershed zone situated between the dual choroidal and retinal circulations located approximately between the outer plexiform layer and the PR inner segments. The precise location of the lowest oxygen tension will vary between scotopic and photopic conditions and with varying degrees of capillary non-perfusion and retinal hypoxia. Figure 5 illustrates the position of this watershed zone.

Larger laser burns allow choroidal oxygen to penetrate further into the inner retina, potentially reaching areas that are not as hypoxic as retinal tissue in the watershed zone. Larger burns may therefore be supplying more oxygen than necessary to those areas. On the other hand, our model suggests smaller burns may help redistribute oxygen from these “oversupplied” areas to “undersupplied” regions within the watershed zone, thereby enhancing oxygenation in the areas that are more vulnerable to hypoxia. Improving oxygenation in the watershed zone, in particular, may be sufficient for mitigating the clinical effects of hypoxia in diabetic retinopathy, without the need for deeper penetration into the inner retina.

The optimum laser spot size and pattern to maximize treatment efficacy while minimizing total burn area remains an open question [17], as the specific retinal oxygenation parameters most relevant to treatment efficacy are still not well understood. However, our model does highlight the importance of considering both the total amount of oxygen and its distribution when evaluating treatment strategies.

Future research should explore the optimum balance between burn size and total retinal burn area to maximize clinical efficacy while minimising retinal damage and preserving visual field. Additionally, whether smaller overall burn areas consisting of smaller individual burns can be as efficacious as current PRP laser practice patterns. This may potentially alter the risk-benefit ratio of treatment and the threshold for laser application.

References

1. Early Treatment Diabetic Retinopathy Study Research Group. Techniques for scatter and local photocoagulation treatment of diabetic retinopathy: Early Treatment Diabetic Retinopathy Study Report no. 3. *International Ophthalmology Clinics. 1987*; 27(4):254-64.
2. Sanghvi C, McLauchlan R, Delgado C, Young L, Charles SJ, Marcellino G, *et al*. Initial experience with the Pascal photocoagulator: a pilot study of 75 procedures. *British Journal of Ophthalmology. 2008*; 92(8):1061-4.
3. Muqit MM, Marcellino GR, Gray JC, Mclauchlan R, Henson DB, Young LB, *et al*. Pain responses of Pascal 20 ms multi-spot and 100 ms single-spot panretinal photocoagulation: Manchester Pascal Study, MAPASS report 2. *British Journal of Ophthalmology. 2010*; 94(11):1493-8.
4. Muqit MM, Denniss J, Nourrit V, Marcellino GR, Henson DB, Schiessl I, *et al.* Spatial and spectral imaging of retinal laser photocoagulation burns. *Investigative ophthalmology & visual science. 2011*; 52(2):994-1002.
5. Royal College of Ophthalmologists Diabetic Retinopathy Guidelines 2012. Accessed August 2023. Available from: https://www.rcophth.ac.uk/wp-content/uploads/2021/08/2012-SCI-267-Diabetic-Retinopathy-Guidelines-December-2012.pdf

6. Nagpal M, Marlecha S, Nagpal K. Comparison of laser photocoagulation for diabetic retinopathy using 532-nm standard laser versus multispot pattern scan laser. *Retina. 2010*; 30(3):452-8.
7. Muraly P, Limbad P, Srinivasan K, Ramasamy K. Single session of Pascal versus multiple sessions of conventional laser for panretinal photocoagulation in proliferative diabetic retinopathy: a comparitive study. *Retina. 2011*;31(7):1359-65.
8. Mirshahi A, Lashay A, Roozbahani M, Fard MA, Molaie S, Mireshghi M, *et al.* Pain score of patients undergoing single spot, short pulse laser versus conventional laser for diabetic retinopathy. *Graefe's Archive for Clinical and Experimental Ophthalmology. 2013;* 251:1103-7.
9. Seymenoğlu RG, Ulusoy MO, Başer EF. Safety and efficacy of panretinal photocoagulation in patients with high-risk proliferative diabetic retinopathy using pattern scan laser versus conventional YAG laser. *The Kaohsiung Journal of Medical Sciences. 2016*; 32(1):22-6.
10. Nemcansky J, Stepanov A, Nemcanska S, Masek P, Langrova H, Studnicka J. Single session of pattern scanning laser versus multiple sessions of conventional laser for panretinal photocoagulation in diabetic retinopathy: efficacy, safety and painfulness. *Plos one. 2019*; 14(7):e0219282.
11. Budzynski E, Smith JH, Bryar P, Birol G, Linsenmeier RA. Effects of photocoagulation on intraretinal PO2 in cat. *Invest Ophthalmol Vis Sci. 2008*; 49(1):380-9.

12. Stefansson E, Landers MB 3rd, Wolbarsht ML. Increased retinal oxygen supply following pan-retinal photocoagulation and vitrectomy and lensectomy. *Trans Am Ophthalmol Soc. 1981*; 79:307-34

13. Wangsa-Wirawan ND, Linsenmeier RA. Retinal Oxygen: Fundamental and Clinical Aspects. *Arch Ophthalmol.* 2003;121(4):547–557

14. R D Braun, R A Linsenmeier, T K Goldstick; Oxygen consumption in the inner and outer retina of the cat.. *Invest. Ophthalmol. Vis. Sci.* 1995;36(3):542-554

15. Linsenmeier RA, Zhang HF. Retinal oxygen: from animals to humans. *Prog Retin Eye Res.* 2017;58:115-15

16. Felder AE, Wanek J, Tan MR, Blair NP, Shahidi M. A Method for Combined Retinal Vascular and Tissue Oxygen Tension Imaging. *Sci Rep*. 2017;7(1):10622

17. National Institute for Health and Care Excellence Diabetic retinopathy guidelines consultation document 2023. Accessed Sept 2023. Available from: https://www.nice.org.uk/guidance/GID-NG10256/documents/evidence-review-12

Figures

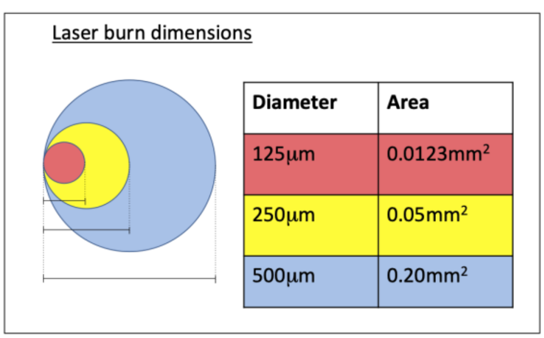

Figure 1. Relationship between burn diameter and burn area

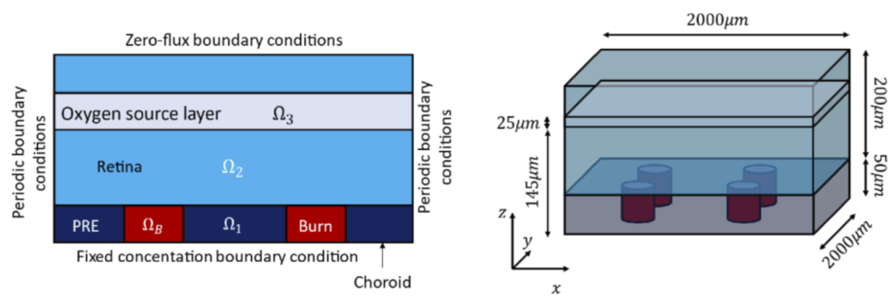

Figure 2. 2D and 3D schematic diagram of mathematical model of choroid, retina and laser burns.

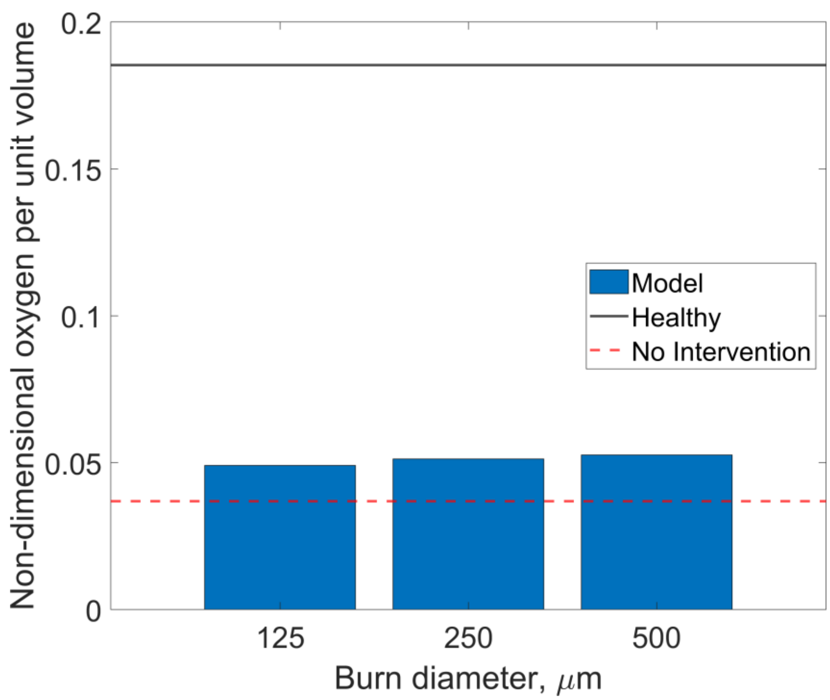

Figure 3. Average retinal oxygen concentration for different burn patterns (500μm, 250μm and 125μm).

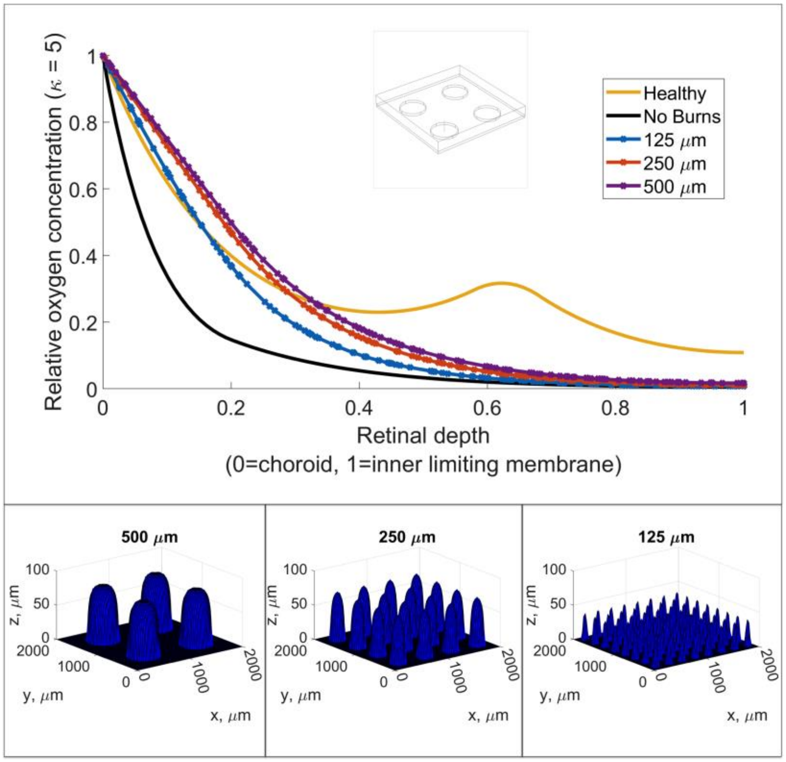

Figure 4. **4A** Oxygen profile through the centre of a single laser burn. **4B** 3D construction of oxygen profiles at all locations in the retinal model. Points show where retinal oxygen matches or exceeds that of the healthy model.

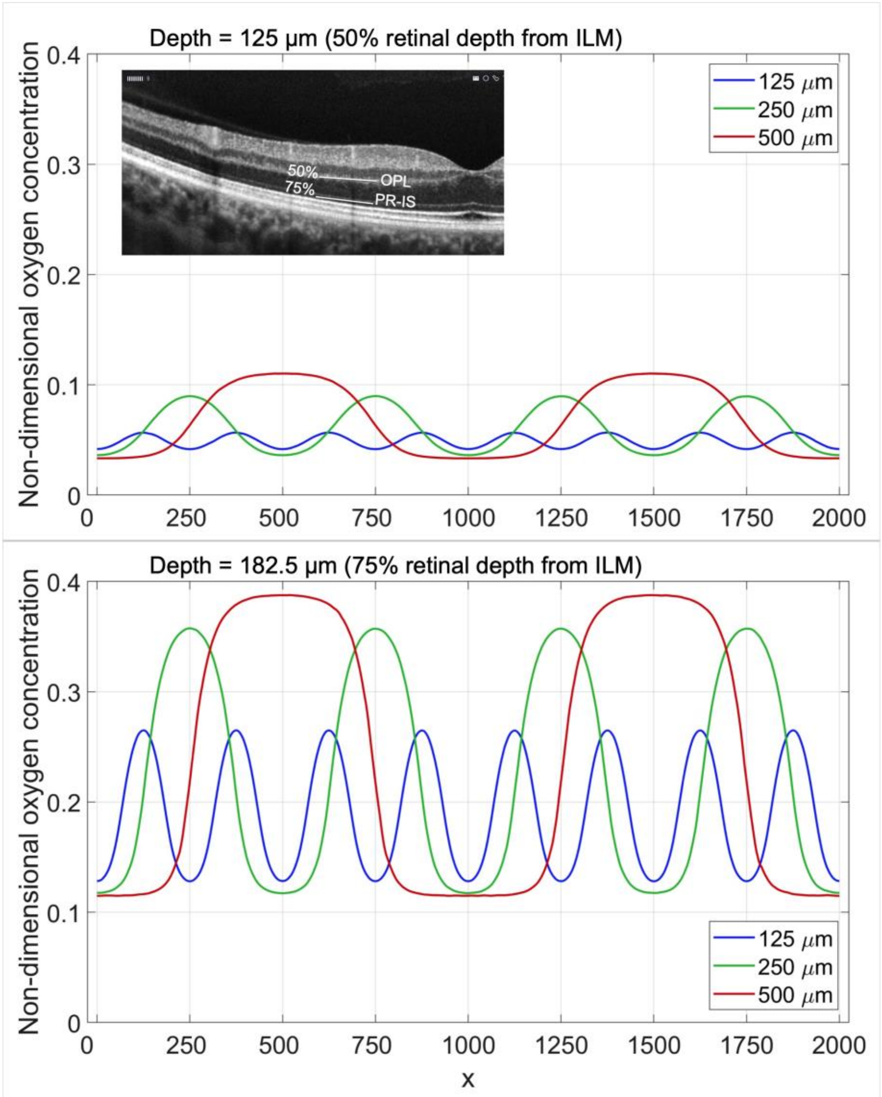

Figure 5. Oxygen concentration along a horizontal line running across a series of burns at a depth (from the ILM) of 50% (125μm) and 75% (182.5μm). Oxygen concentration is highest over the centre of a burn and decreases with increasing eccentricity from the burn. (Inset: OCT scan showing approximate anatomical locations (50% depth - OPL (outer plexiform layer), 75% depth – PR-IS (Photoreceptor inner segments), W – watershed zone between retinal and choroidal circulations.)

Supplementary file 1

Technical methods

Let u be the nondimensionalised oxygen concentration in the $2000\mu m \times 2000\mu m \times 250\mu m$ cuboid then u satisfies the diffusion degradation equation everywhere [1,2],

$$\frac{\partial u}{\partial t} = \mathrm{D}\nabla^2 u - \gamma(x, y, z)u + s(z).$$

where the degradation rate, $\gamma(x, y, z)$, and source term, s, are spatially dependent on the domain, Ω_i, see Figure S1. We use the nondimensionalised form of u as the provided data is normalised to be a percentage. Thus, the quantitative size is irrelevant. Only ratios of solutions are important.

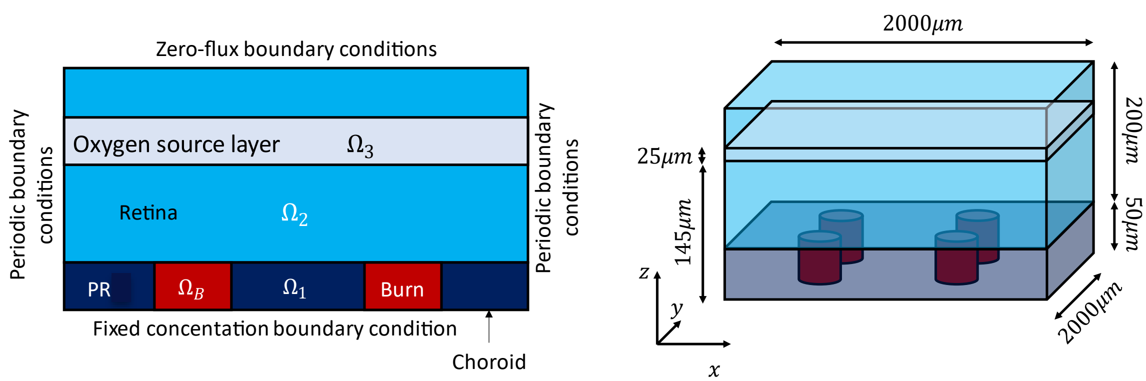

Figure S1. 2D and 3D schematic diagram of mathematical model of choroid, retina and laser burns

Specifically,

$$\gamma(x,y,z) = \begin{cases} \hat{\gamma}\ when\ (x,y,z) \in \Omega_2 \cup\ \Omega_3, \\ 5\hat{\gamma}\ when\ (x,y,z) \in \Omega_1, \\ 0\ when\ (x,y) \in \Omega_B, \end{cases}$$

$$s = \begin{cases} \hat{s}\ \ when\ z \in \Omega_3\ and\ the\ tissue\ is\ healthy, \\ 0\ otherwise, \end{cases}$$

and the parameter values are $D = 6.25 \times 10^{-5} cm^2/s, \hat{\gamma} = 25000/s$, and $\hat{s} = 30000/s$. The diffusion coefficient is of the right order of magnitude, as measured [3]. The sink and source values where then chosen to be of the correct order to reproduce the observations in [4]. Although the values should be treated as predictions, they are of the same order as parameters used in other recent modelling work [5].

For the boundary conditions $u = 1$ on $z = 0$ (fixed concentration), $u(0, y, z, t) = u(2000, y, z, t)$ and $u(x, 0, z, t) = u(x, 2000, z, t)$ (periodic boundary conditions) and $\partial u/\partial z = 0$ on $z = 250$ (zero-flux boundary condition). The initial condition is $u = 0$ almost everywhere at $t = 0$.

Since we are using COMSOL Multiphysics 6 to create the 3D simulations we do not have direct access to the mesh size. Instead, we can specify a maximum element size, meaning that no side length of the tetrahedrons that discretise the domain are longer than the given value. However, software's meshing algorithm refines the mesh in regions where there are sharp geometry transitions, such as around the burn holes.

In Figure S2 we calculate the average u value over all space for different maximum element sizes. Specifically, we are simulating the case that the burn holes are separated by 125 μm (the simulation shown in the right of 4B), which is the simulation that has the largest number of sharp gradients and, thus, is most prone to errors. For all maximum element sizes less than 40μm the difference between evaluated values is less than 10^{-4}

and less than 10^{-6} maximum element sizes less than $30\mu m$. Since all of our simulations use a maximum element sizes of $20\mu m$, we can be confident in the accuracy of the solution. Note, that due to computational limitations we could not drop the maximum element size lower than $10\mu m$. Thus, $20\mu m$ was chosen as a trade off between accuracy and speed of simulation.

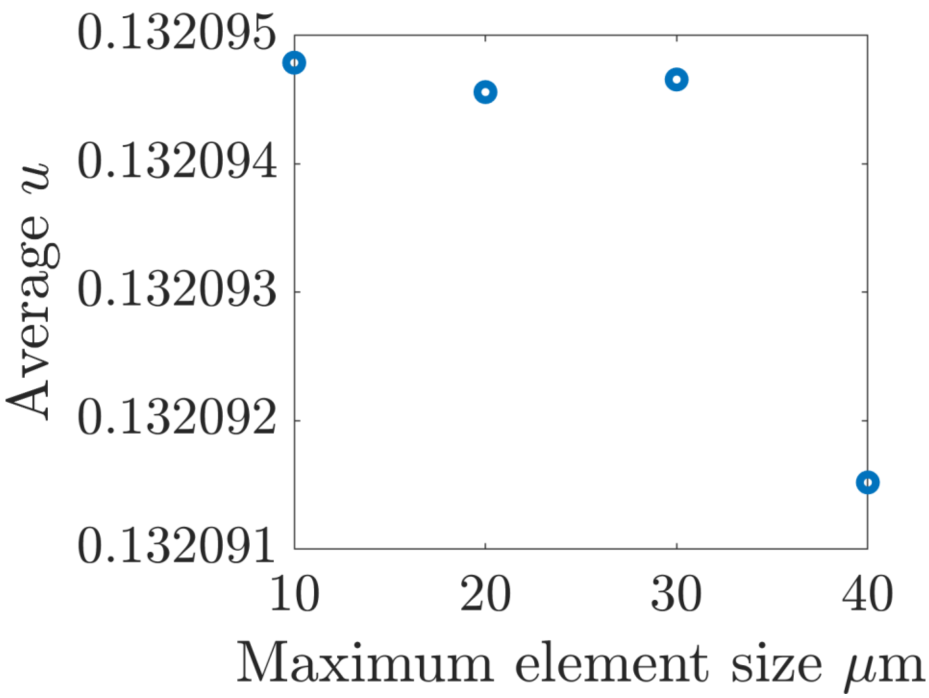

[1] Murray, James D. "Mathematical biology II: Spatial models and biomedical applications." *Monographs on Applied and Computational Mathematics* 3 (1973).

[2] Woolley, T. E., Baker, R. E., Tickle, C., Maini, P. K., & Towers, M. (2014). Mathematical modelling of digit specification by a sonic hedgehog gradient. *Developmental Dynamics*, *243*(2), 290-298.

[3] Linsenmeier R. A., Zhang H. F. Retinal oxygen: from animals to humans. Prog Retin Eye Res. 2017 May;58:115-151. doi: 10.1016/j.preteyeres.2017.01.003. Epub 2017 Jan 18. PMID: 28109737; PMCID: PMC5441959.

[4] Wangsa-Wirawan N. D., Linsenmeier R. A. Retinal Oxygen: Fundamental and Clinical Aspects. *Arch Ophthalmol.* 2003;121(4):547–557. doi:10.1001/archopht.121.4.547

[5] Seth, D., Mishra, K. P., Ghai, R., Mishra, R., & Kumar, A. (2022). Mathematical model for oxygen diffusion in the retina. *Materials Today: Proceedings*, *57*, 2372-2375.

Healthy model comparison graph

In the model of the retinal oxygen profile, the choroid as an oxygen source was present in both the DR model and the healthy model. In the healthy model, an additional oxygen source was inserted at a depth beginning at 80 microns and extending for 25 microns. This layer is a simplified approximation of the inner retinal capillary plexuses. The graph below shows comparison of the healthy model oxygen profile with reference data taken from: Wangsa-Wirawan ND, Linsenmeier RA. Retinal Oxygen: Fundamental and Clinical Aspects. *Arch Ophthalmol.* 2003;121(4):547–557